RAPID COMMUNICATIONS

PHYSICAL REVIEW B **81**, 020509(R) (2010)

# Weak anisotropy of the superconducting upper critical field in $Fe_{1.11}Te_{0.6}Se_{0.4}$ single crystals

Minghu Fang,[1] Jinhu Yang,[1] F. F. Balakirev,[2] Y. Kohama,[2] J. Singleton,[2] B. Qian,[3] Z. Q. Mao,[3] Hangdong Wang,[1] and H. Q. Yuan[1,*]

[1]*Department of Physics, Zhejiang University, Hangzhou, Zhejiang 310027, China*
[2]*NHMFL, Los Alamos National Laboratory, MS E536, Los Alamos, New Mexico 87545, USA*
[3]*Department of Physics, Tulane University, New Orleans, Louisiana 70118, USA*

(Received 19 October 2009; revised manuscript received 22 December 2009; published 27 January 2010)

We have determined the resistive upper critical field $H_{c2}$ for single crystals of the superconductor $Fe_{1.11}Te_{0.6}Se_{0.4}$ using pulsed magnetic fields of up to 60 T. A rather high zero-temperature upper critical field of $\mu_0 H_{c2}(0) \approx 47$ T is obtained in spite of the relatively low superconducting transition temperature ($T_c \approx 14$ K). Moreover, $H_{c2}$ follows an unusual temperature dependence, becoming almost independent of the magnetic field orientation as the temperature $T \to 0$. We suggest that the isotropic superconductivity in $Fe_{1.11}Te_{0.6}Se_{0.4}$ is a consequence of its three-dimensional Fermi-surface topology. An analogous result was obtained for $(Ba,K)Fe_2As_2$, indicating that all layered iron-based superconductors exhibit generic behavior that is significantly different from that of the "high-$T_c$" cuprates.

DOI: 10.1103/PhysRevB.81.020509 PACS number(s): 74.70.Xa, 71.35.Ji, 74.25.Op

The discovery of superconductivity in the iron pnictides $R$FeAs(O,F) (where $R$ can be La, Ce, Pr, Nd, Sm, or Gd)[1–5] with transition temperatures $T_c$ as high as 55 K has been responsible for something of a resurrection in the study of high-temperature superconductivity. Beside the $R$FeAs(O,F) series (the so-called "1111s"), other families of the iron-based superconductors have been found, including the "122" materials possessing the $ThCr_2Si_2$ structure (e.g., hole- or electron-doped $BaFe_2As_2$),[6,7] the "111-type" LiFeAs family[8,9] and the "11-type" iron chalcogenides with an $\alpha$-PbO structure [e.g., $Fe_{1+x}$(Se,Te) (Refs. 10 and 11)]. All of these compounds share a common structural feature, i.e., square planar sheets of Fe, coordinated tetrahedrally by pnictogens or chalcogens. The relatively high superconducting transition temperatures and layered crystal structures of the Fe-based superconductors initially suggested strong analogies with the cuprates. However, in this Rapid Communication we report pulsed-field magnetoresistance measurements for single crystals of $Fe_{1.11}Te_{0.6}Se_{0.4}$ that show that its upper critical field attains a value of 47 T as temperature $T \to 0$ that is almost independent of field direction. This suggests that the electronic properties of $Fe_{1+x}$(Te,Se) superconductors are rather isotropic (i.e., three dimensional), in complete contrast to those of the quasi-two-dimensional cuprates. A similar effect was found in $(Ba,K)Fe_2As_2$ (Ref. 12) and other 122-type systems,[13–15] indicating that this may be a general feature of *all* iron pnictides.

Large single crystals of $Fe_{1.11}Te_{0.6}Se_{0.4}$ were grown by a self-flux method. The starting composition was $Fe(Te_{0.6}Se_{0.4})_{0.85}$. The mixtures of Fe and (Te,Se) were ground thoroughly and sealed in an evacuated quartz tube. The tube was heated to 920 °C and cooled slowly to grow large single crystals. The crystals obtained were checked by x-ray diffraction (XRD); their composition was analyzed using a scanning electron microscope (Hitachi S3400) equipped with an energy dispersive x-ray spectrometer (EDXS). Longitudinal resistivity was measured using a typical four-contact method in pulsed fields of up to 60 T at the National High Magnetic Field Laboratory, Los Alamos.[12] In order to minimize inductive self-heating caused by the pulsed magnetic field, small crystals with typical sizes $2 \times 0.5 \times 0.1$ mm$^3$ were cleaved off along the $c$ direction from the as-grown samples. Data were recorded using a 10 MHz digitizer and 100 kHz alternating current and analyzed using a custom low-noise digital lock-in technique.[12] Care was taken to ensure that neither the current nor the field pulse caused significant heating. The temperature dependence of the resistivity at zero field was measured with a Lakeshore resistance bridge. Complementary magnetization data $M(T)$ were measured using a Quantum Design superconducting quantum interference device (SQUID) magnetometer.

Figure 1 presents the temperature dependence of the in-plane electrical resistivity $\rho_{ab}(T)$ for $Fe_{1.11}Te_{0.6}Se_{0.4}$ at zero field. As reported in the literature,[16,17] $Fe_{1.11}Te_{0.6}Se_{0.4}$ exhibits a resistivity that increases with decreasing temperature. Nevertheless, it undergoes a relatively sharp superconducting transition at $T_c = 14 \pm 0.3$ K, which is further confirmed by the temperature dependence of the dc magnetic susceptibility, as shown in the inset of Fig. 1. It is noted that the superconducting transition seen in the magnetic susceptibility becomes shaper with reducing the magnetic field.

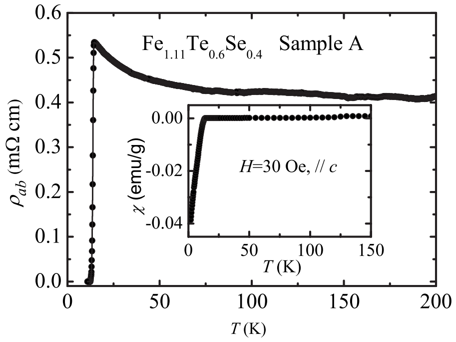

FIG. 1. (a) Temperature dependence of the in-plane resistivity $\rho_{ab}(T)$ at zero field for $Fe_{1.11}Te_{0.6}Se_{0.4}$ single crystals. The inset shows dc magnetic susceptibility $\chi(T)$ measured at 30 Oe with zero field cooling process. Both resistivity and magnetic susceptibility indicate a superconducting transition at $T_c \approx 14$ K.

1098-0121/2010/81(2)/020509(4)

©2010 The American Physical Society

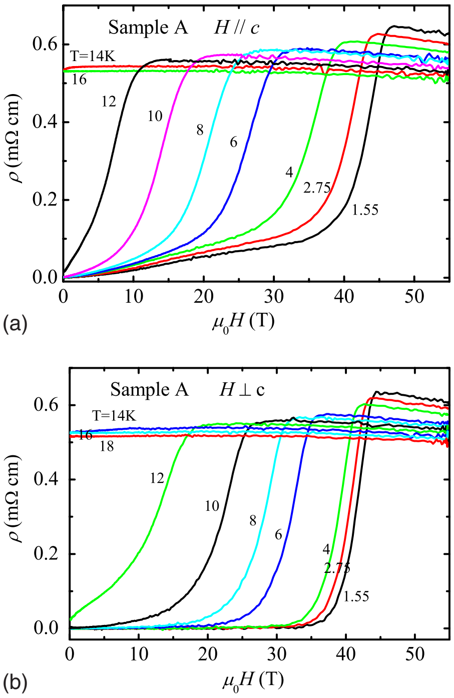

FIG. 2. (Color online) The field dependence of the electrical resistivity $\rho_{ab}$(H) at various temperatures for $Fe_{1.11}Te_{0.6}Se_{0.4}$. (a) $H \| c$ and (b) $H \perp c$.

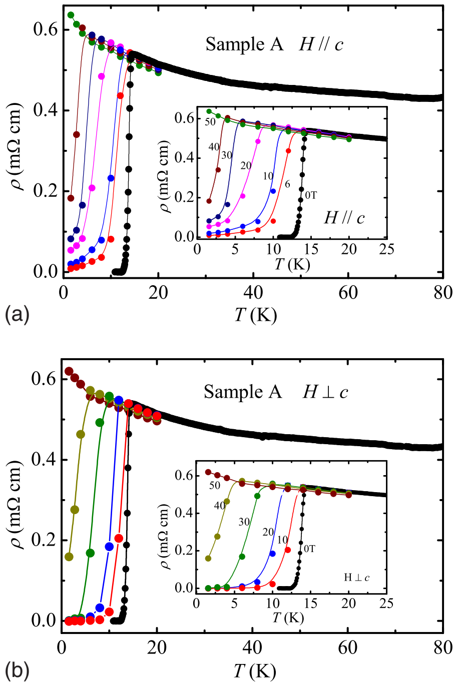

FIG. 3. (Color online) The electrical resistivity versus temperature at selected magnetic fields. (a) $H \| c$ and (b)$H \perp c$ axis. The insets plot the superconducting transitions in detail.

The field-dependent electrical resistivity, $\rho(H)$, at various temperatures is shown in Figs. 2(a) and 2(b) for magnetic fields applied parallel ($H \| c$) and perpendicular to ($H \perp c$) the $c$ axis, respectively. For consistency, only data collected during the down sweep of the magnet are shown. The superconducting to normal transition is visible as a sharp rise in $\rho$; inside the superconducting state, an apparent finite $\rho$ is observed for $H \| c$ but not for $H \perp c$. The former behavior is likely to be due to dissipation associated with thermally activated flux motion.[18] Nevertheless, it is obvious that at the same temperature, superconductivity is suppressed by similar values of the magnetic field applied parallel or perpendicular to the $c$ axis.

Figure 3 shows the temperature dependence of the resistivity for various magnetic fields. For a field of 50 T, the superconductivity is suppressed at all temperatures, revealing a normal-state resistivity that increases monotonically with decreasing temperature for both $H \| c$ and $H \perp c$. This continues the "insulating" trend seen at higher temperatures (Fig. 1) which has been attributed to weak charge carrier localization due to the excess Fe.[17] However, it should be noted that a weak metal-insulator-like crossover is also observed at cryogenic temperatures in some underdoped iron pnictides when superconductivity is suppressed by a large magnetic field,[12,19] suggesting that this behavior might be a more general phenomenon that is not primarily associated with excess Fe in $Fe_{1.11}Te_{0.6}Se_{0.4}$.

The temperature dependence of the upper critical field ($H_{c2}$) of $Fe_{1.11}Te_{0.6}Se_{0.4}$ determined from the mid-point of the resistive superconducting transitions, as shown in Fig. 2, is plotted in Fig. 4 for magnetic field parallel and perpendicular to the $c$ axis. The error bars mark the fields at 20% and 80% drops of the normal-state resistivity just above $T_c$. We note that the relatively large error bars for $H \| c$ originate from the none-zero resistance below $T_c$, an effect likely due to flux motion as mentioned above. The two crystals (samples A and B, with $T_c = 14 \pm 0.3$ K) exhibit an almost identical behavior of $H_{c2}$, indicating good sample reproducibility. The most remarkable aspect of Fig. 4 is the fact that the upper critical fields of $Fe_{1.11}Te_{0.6}Se_{0.4}$ for the two field orientations merge together as $T \rightarrow 0$ at $\mu_0 H_{c2} \approx 47$ T. This $H_{c2}(0)$ is consistent with the value determined for the polycrystalline sample.[20]

The anisotropy coefficient $\gamma(T)$ determined from $\gamma(T) = H_{c2}^{\perp}/H_{c2}^{\|}$ decreases monotonically from 2 near $T = T_c$ to

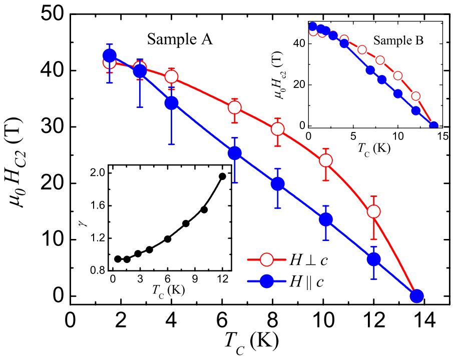

FIG. 4. (Color online) Temperature dependence of the upper critical field for sample A (main plot) and sample B (upper inset) where the solid and open symbols represent $H \| c$ and $H \perp c$, respectively. These data sets indicate good sample reproducibility of $H_{c2}(Tc)$. The lower inset plots the anisotropic coefficient $\gamma(= H_{c2}^{\perp}/H_{c2}^{\|})$ as a function of temperature for sample B.

about 0.95 at $T=0$ (see the lower inset of Fig. 4). Similar isotropic behavior of the upper critical field has also been observed in the 122 series of Fe-based superconductors.[12–15] All these results indicate that nearly isotropic superconductivity might be a general, but very unique feature, of the iron-based superconductors.

The anisotropy of the upper critical field is usually determined by the underlying electronic band structure. In the layered cuprates and organic superconductors, the Fermi surfaces are rather two dimensional.[21,22] As a result, there is considerable anisotropy; the upper critical field of these materials is large for in-plane fields, being determined by spin mechanisms such as the Pauli paramagnetic limit, but generally much smaller and restricted by orbital mechanisms for other field orientations.[23,24] However, the experiments in this Rapid Communication show that this is *not* the case for $Fe_{1.11}Te_{0.6}Se_{0.4}$; its upper critical field $H_{c2}$ at low temperature displays only a very weak dependence on magnetic field orientation (see Fig. 4). By contrast, calculations indicate that the iron pnictides and chalcogenides have much more three-dimensional band structures.[25–27] While the layered crystal structure is reflected in the generally cylindrical shapes of the Fermi-surface sections, there is very pronounced dispersion in the $k_z$ direction, leading to strong warping, seen both in the theoretical predictions[25–27] and in angle resolved photon emission spectroscopy (ARPES) data;[28] by contrast, there is very little warping in the cuprates[21] and organics.[22] We argued in Ref. 12 that the nearly isotropic superconductivity observed in $(Ba,K)Fe_2As_2$ probably reflects the three-dimensional nature of the Fermi surface. The $\alpha$-Fe(Se,Te) system has the simplest crystal structure of all the Fe-based superconductors, comprising a continuous stack of tetrahedral Fe(Se,Te) layers along the $c$ axis; consequently, it is expected that the Fermi surface will also be three dimensional in nature, leading naturally to the weak anisotropy of $H_{c2}$ seen here in $Fe_{1.11}Te_{0.6}Se_{0.4}$. Therefore, the remarkable lack of anisotropy in $H_{c2}$ observed in both the 122- and 11-type iron superconductors has a common origin. In the iron-based superconductors, the coupling between the FeAs or Fe(Te, Se) layers would play an important role and cannot be neglected, which is quite distinct from the cuprates in terms of effective dimensionality.

Although the low-temperature upper critical field is rather isotropic, the initial slope of $H_{c2}$ near $T_c$ does show some dependence on the field orientation (Fig. 4); similar behavior in the 122 compounds has been attributed to two-band superconductivity.[13] In our resistive critical field data, $dH_{c2}/dT(T=T_c)$ is about 8.90 T/K for $H\perp c$ and 3.82 T/K for $H\parallel c$, respectively. These are close to the values observed for $Fe_{1.11}Te_{0.6}Se_{0.4}$ in dc field measurements.[16,20] Upon cooling down, $H_{c2}(T)$ for $H\perp c$ starts to bend down, resulting in a significantly lower zero temperature upper critical field compared to typical extrapolation methods. For example, the upper critical field at $T=0$ determined by the Werthamer-Helfand-Hohenberg (WHH) theory[29] yields a value of about 87 T for $H\perp c$ (sample A), a much higher value than the actually measured 47 T. It is noted that the multiband nature of $Fe_{1.11}Te_{0.6}Se_{0.4}$ may cause a deviation of $H_{c2}(T)$ from WHH theory. From this experimental value of $H_{c2}(0)$, one can calculate the superconducting coherence length of $Fe_{1.11}Te_{0.6}Se_{0.4}$ as 2.65 nm.

In summary, we have determined the resistive upper critical field of $Fe_{1.11}Te_{0.6}Se_{0.4}$ single crystals for fields applied both parallel and perpendicular to the $c$ direction. It is found that the anisotropy of the upper critical field decreases with decreasing temperature, becoming rather isotropic at low temperature ($\mu_0H_{c2}(0\text{ K})\approx 47$ T). Similar behavior was also observed in the 122-type iron pnictides.[12–15] The nearly isotropic superconductivity shown in these layered compounds is probably attributable to the unique three-dimensional nature of their Fermi-surface topology. This is in great contrast to the cases of high $T_c$ cuprates and organic superconductors which possess highly anisotropic upper critical fields due to their quasi-two-dimensional band structure. As pointed out in Ref. 30, our findings of isotropic superconductivity together with a rather high upper critical field suggest that the iron-based superconductors are very promising materials for future applications, in particular if $T_c$ could be further enhanced above liquid nitrogen temperature.

This work was supported by the National Science Foundation of China, the National Basic Research Program of China (973 program), the PCSIRT of the Ministry of Education of China, Zhejiang Provincial Natural Science Foundation of China, the DOE BES program "Science in 100 T" and the NHMFL-UCGP. Work at NHMFL-LANL is performed under the auspices of the National Science Foundation, Department of Energy and State of Florida.

---

*hqyuan@zju.edu.cn

[1] Y. Kamihara, T. Watanabe, M. Hirano, and H. Hosono, J. Am. Chem. Soc. **130**, 3296 (2008).

[2] X. H. Chen, T. Wu, G. Wu, R. H. Liu, H. Chen, and D. F. Fang, Nature (London) **453**, 761 (2008).

[3] G. F. Chen, Z. Li, D. Wu, G. Li, W. Z. Hu, J. Dong, P. Zheng, J. L. Luo, and N. L. Wang, Phys. Rev. Lett. **100**, 247002 (2008).

[4] H. H. Wen, G. Mu, L. Fang, H. Yang, and X. Zhu, EPL **82**, 17009 (2008).

[5] Z. A. Ren, W. Lu, J. Yang, W. Yi, X. L. Shen, Z. C. Li, G. C. Che, X. L. Dong, L. L. Sun, F. Zhou, and Z. X. Zhao, Chin. Phys. Lett. **25**, 2215 (2008).

[6] M. Rotter, M. Tegel, and D. Johrendt, Phys. Rev. Lett. **101**, 107006 (2008).

[7] A. S. Sefat, R. Jin, M. A. McGuire, B. C. Sales, D. J. Singh, and D. Mandrus, Phys. Rev. Lett. **101**, 117004 (2008).

[8] X. C. Wang, Q. Q. Liu, Y. X. Lv, W. B. Gao, L. X. Yang, R. C. Yu, F. Y. Li, and C. Q. Jin, Solid State Commun. **148**, 538 (2008).

[9] M. J. Pitcher, D. R. Parker, P. Adamson, S. J. C. Herkelrath, A. T. Boothroyd, and S. J. Clarke, Chem. Commun. (Cambridge) **2008**, 5918.

[10] F.-C. Hsu, J.-Y. Luo, K.-W. Yeh, T.-K. Chu, D.-C. Yan, and M. K. Wu, Proc. Natl. Acad. Sci. U.S.A. **105**, 14262 (2008).

[11] M. H. Fang, H. M. Pham, B. Qian, T. J. Liu, E. K. Vehstedt, Y. Liu, L. Spinu, and Z. Q. Mao, Phys. Rev. B **78**, 224503 (2008).

[12] H. Q. Yuan, J. Singleton, F. F. Balakirev, S. A. Baily, G. F. Chen, J. L. Luo, and N. L. Wang, Nature (London) **457**, 565 (2009).

[13] S. A. Baily, Y. Kohama, H. Hiramatsu, B. Maiorov, F. F. Balakirev, M. Hirano, and H. Hosono, Phys. Rev. Lett. **102**, 117004 (2009).

[14] M. M. Altarawneh, K. Collar, C. H. Mielke, N. Ni, S. L. Bud'ko, and P. C. Canfield, Phys. Rev. B **78**, 220505(R)(2008).

[15] M. Kano, Y. Kohama, D. Graf, F. F. Balakirev, A. S. Sefat, M. A. McGuire, B. C. Sales, D. Mandrus, and S. W. Tozer, J. Phys. Soc. Jpn. **78**, 084719 (2009).

[16] G. F. Chen, Z. G. Chen, J. Dong, W. Z. Hu, G. Li, X. D. Zhang, P. Zheng, J. L. Luo, and N. L. Wang, Phys. Rev. B **79**, 140509(R) (2009).

[17] T. J. Liu, X. Ke, B. Qian, J. Hu, D. Fobes, E. K. Vehstedt, H. Pham, J. H. Yang, M. H. Fang, L. Spinu, P. Schiffer, Y. Liu, and Z. Q. Mao, Phys. Rev. B **80**, 174509 (2009).

[18] M. Tinkham, *Introduction to Superconductivity* (McGraw-Hill, New York, 1975).

[19] S. C. Riggs, J. B. Kemper, Y. Jo, Z. Stegen, L. Balicas, G. S. Boebinger, F. F. Balakirev, A. Migliori, H. Chen, R. H. Liu, and X. H. Chen, Phys. Rev. B **79**, 212510 (2009).

[20] T. Kida, T. Matsunaga, M. Hagiwara, Y. Mizuguchi, Y. Takano, and K. Kindo, J. Phys. Soc. Jpn. **78**, 113701 (2009).

[21] S. E. Sebastian, N. Harrison, E. Palm, T. P. Murphy, C. H. Mielke, R. Liang, D. A. Bonn, W. N. Hardy, and G. G. Lonzarich, Nature (London) **454**, 200 (2008).

[22] P. A. Goddard, S. J. Blundell, J. Singleton, R. D. McDonald, A. Ardavan, A. Narduzzo, J. A. Schlueter, A. M. Kini, and T. Sasaki, Phys. Rev. B **69**, 174509 (2004).

[23] J. Brooks and J. R. Shriffer, *Handbook of High Temperature Superconductivity* (Springer, New York, 2006).

[24] J. Singleton and C. Mielke, Contemp. Phys. **43**, 63 (2002).

[25] A. Subedi, L. J. Zhang, D. J. Singh, and M. H. Du, Phys. Rev. B **78**, 134514 (2008).

[26] F. J. Ma, Z. Y. Lu, and T. Xiang, arXiv:0806.3526, Front. Phys. China (to be published).

[27] I. I. Mazin, M. D. Johannes, L. Boeri, K. Koepernik, and D. J. Singh, Phys. Rev. B **78**, 085104 (2008).

[28] P. Vilmercati, A. Fedorov, I. Vobornik, U. Manju, G. Panaccione, A. Goldoni, A. S. Sefat, M. A. McGuire, B. C. Sales, R. Jin, D. Mandrus, D. J. Singh, and N. Mannella, Phys. Rev. B **79**, 220503(R)(2009).

[29] N. R. Werthamer, E. Helfand, and P. C. Hohenberg, Phys. Rev. **147**, 295 (1966).

[30] M. R. Norman, Physics **1**, 21 (2008).